Application Report

Waveform Capture Based Ultrasonic Sensing Water Flow Metering Technology

Srinivas Lingam and Anand Dabak

MSP430 System Applications

ABSTRACT

This application report describes the time-of-flight (TOF) approach for water flow measurement using ultrasonic sensing (USS) technology. Topics include the general principles behind flow rate estimation and a block diagram of the signal chain. This information is the basis of the software implementation of the waveform capture based ultrasonic algorithms on the MSP430FR604x microcontrollers (MCUs).

Table of Contents

List of Figures

Trademarks

All trademarks are the property of their respective owners.

1 Flow Metering Background

This document describes the ultrasonic time-of-flight (TOF) based algorithms for water flow measurement. Figure 1-1 shows different configurations that are used in practice for the ultrasonic TOF technique.

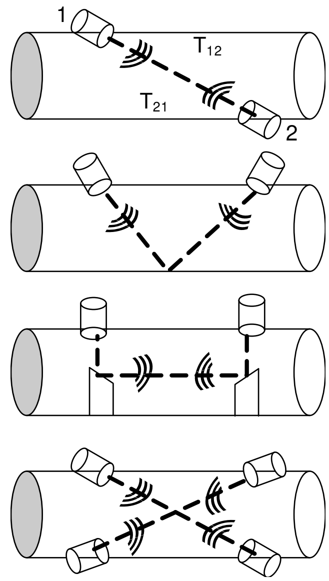

Figure 1-1. Configurations for Ultrasonic TOF Based Measurement

This document uses the structure in Figure 1-2 for analysis of ultrasonic TOF techniques.

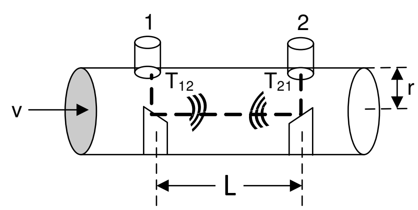

Figure 1-2. Transmit and Receive Transducers for Ultrasonic Measurements

In Figure 1-2, the two transducers are numbered 1 and 2, T_{12} is the propagation time for the ultrasonic signal from transducer 1 to 2, and T_{21} is the propagation time for the signal from transducer 2 to 1. Equation 1 and Equation 2 calculate the propagation times in the two directions as a function of the velocity of ultrasound in water and the velocity of water flow. The parameters in the equation are c = velocity of ultrasound in water, v = velocity of water flow, and L = the propagation length of the pipe along the flow of water. Because this length is much larger than the radius r of the pipe, the propagation length of the wave perpendicular to the flow is neglected in this analysis.

$$T_{12} = \frac{L}{c + v} \tag{1}$$

$$T_{21} = \frac{L}{c - v} \tag{2}$$

The objective is to solve for the velocity v of the water flow so that can be used to indicate the water flow volume which would be given by volume = A × v, with the assumption that the cross sectional area A of the pipe is known.

Equation 3 calculates the differential TOF of the upstream and downstream signals.

$$\Delta T = T_{21} - T_{12} \tag{3}$$

1.1 Water Flow Velocity Estimation

There are two methods to solve Equation 1 and Equation 2. One method can be used when the velocity of ultrasound in water is known (see Section 1.1.1), and the other method can be used when the velocity of ultrasound in water is not known (see Section 1.1.2).

1.1.1 Velocity of Ultrasound in Water is Known

When the velocity c of ultrasound in water is known, Equation 4 uses this velocity to solve for the water flow velocity v.

$$\Delta T = T_{21} - T_{12} = \frac{2Lv}{c^2 - v^2} \tag{4}$$

However, the velocity c of ultrasound in water is a function of temperature. Based on the data in Figure 1-3, Equation 5 gives a first-order simple expression for the dependence of ultrasound velocity in water. The temperature in the equation is in degrees Celsius (°C).

$$c = 1404.3 + 4.7T_{temp} - 0.04T_{temp}^2 \tag{5}$$

Figure 1-3 shows the change of velocity c of ultrasound in water as a function of temperature.

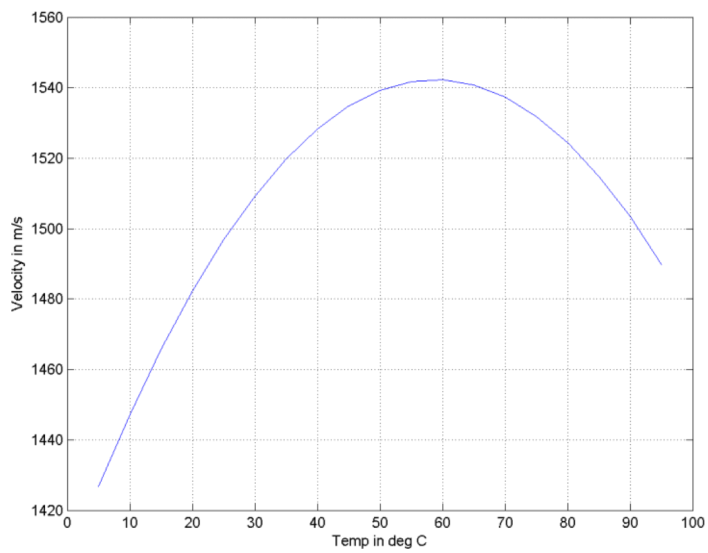

Figure 1-3. Velocity of Ultrasound in Water as a Function of Water Temperature

If the water meter does not take this temperature dependence into account and only assumes a nominal 25°C temperature, an error of up to ±3.5% can occur in the absolute time-of-flight estimation. Therefore, a temperature sensor is needed for the estimation of velocity c of ultrasound in water using Equation 4.

1.1.2 Velocity of Ultrasound in Water is Unknown

If the velocity of ultrasound in water is unknown, Equation 6 can be used to solve for the velocity of the water flow.

$$v = \frac{L}{2} \times \left(\frac{1}{T_{12}} - \frac{1}{T_{21}}\right) = \frac{L}{2} \times \frac{T_{21} - T_{12}}{T_{21}T_{12}} = \frac{L}{2} \times \frac{\Delta T}{T_{21}T_{12}} \tag{6}$$

This equation needs the propagation times [or absolute times of flight (AbsTOF)] T_{12} and T_{21} in the two directions along the cross section of the pipe. The TI solution implements this technique so that the velocity of sound in water is not required for accurate measurement of water flow velocity.

2 Algorithms for Ultrasonic Water Flow Metering

In both of the methods described in Section 1.1.1 and Section 1.1.2 the knowledge of the differential TOF as given in Equation 3 is required. There are two techniques for differential TOF measurement:

- Zero-crossing based using a time-to-digital converter (TDC): This technique uses an initial threshold crossing for the signal, followed by zero crossings of the signal

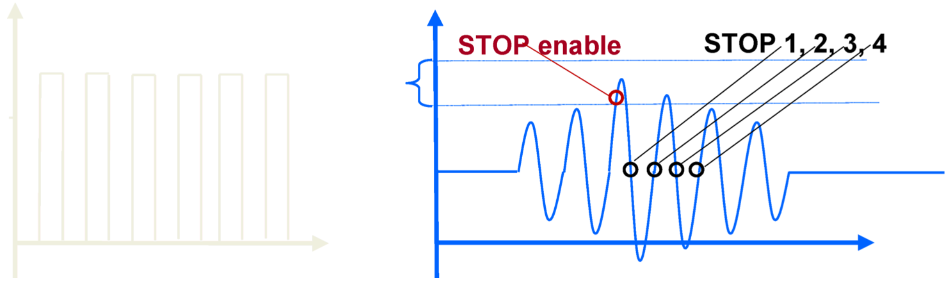

Figure 2-1. Zero-Crossing Based Time-to-Digital Converter

- Correlation based using an analog-to-digital converter (ADC): In this technique the whole waveform is captured using ADC and stored for the up/dn stream and then post processing is done on the waveform to derive the differential time of flight.

This document describes the ADC-based technique for ultrasonic flow metering. This approach was chosen because of the following advantages over TDC techniques:

- Performance: The correlation acts as a digital filter to suppress noise (implemented efficiently on the low energy accelerator (LEA) on the MSP430FR6047 MCU). This results in 3 to 4 times lower noise standard deviation. The correlation filter also suppresses other interference like line noise.
- Robustness to signal amplitude variations: The algorithm is insensitive to the received signal amplitude as can occur with high flow rates, transducer-to-transducer variation, and temperature variation.
- The envelope of the signal is obtained naturally in ADC-based processing: This enables tuning to the transducer frequencies because slow variations in the envelope across time can be used to detect aging of transducers or meters.

2.1 Correlation Based Technique for Differential TOF Estimation

The correlation based TOF estimation involves the following steps:

1. A pulse is transmitted from transducer 1 in Figure 1-2.
2. Immediately a clock counter is started with respect to the reference clock. The reference clock can be either 8 or 16 MHz.
3. At a certain pre-determined time, the ADC is started to capture the data at the receive transducer. Let the received data be indicated as Equation 7.

$$\bar{r}_2 = \{r_2^1, r_2^2, r_2^3, \ldots, r_2^N\} \tag{7}$$

   where

   - $r_1^i = r_2\left(\frac{i}{f_s}\right)$
   - f_s = sampling rate of the ADC
   - i = index of the sample

4. Similarly, transmit the pulse from transducer 2 and receive the signal at the transducer. Let the sampled signal at transducer 1 be given by Equation 8.

$$\bar{r}_1 = \{r_1^1, r_1^2, r_1^3, \ldots, r_1^N\} \tag{8}$$

5. Based on $\bar{r}_1$ and $\bar{r}_2$, a correlation value is calculated by Equation 9.

$$\text{corr}(k) = \sum_{i=1}^{N} r_1^{i+k} r_2^{k} \quad (9)$$

where

- $k = \{-m, -(m-1), \ldots, (m-1), m\}$
- $r_1^i, r_2^i = 0$ for $i < 1$ and $i > N$

6. The maximum of the correlation is calculated by Equation 10.

$$\hat{k} = \max_k(\text{corr}(k)) \quad (10)$$

7. Let $Z_{-1} = \text{corr}(\hat{k}-1)$, $Z_0 = \text{corr}(\hat{k})$, and $Z_1 = \text{corr}(\hat{k}+1)$ be the values of correlation at and around the maximum.
8. The real maximum of the correlation is now given by the interpolation in Equation 11.

$$\delta = interp_{max}[Z_{-1}, Z_0, Z_1] \quad (11)$$

9. The net different time of flight is now given by Equation 12.

$$T_{12}^{corr} = (\hat{k} - m + \delta) \quad (12)$$

10. In USS Software Library implementations, m is typically chosen to be +1, implying that only 3 correlations must be computed most of the time.

This correlation-based TOF calculation has been reported in the literature previously as given in 2 and 3. The details of the equations for δ in Equation 12 can be found in 4 and provided in Section 2.2.1 for completeness. Figure 2-2 shows a block diagram of the receiver for the correlation. Figure 2-3 shows a block diagram of the signal processing algorithms.

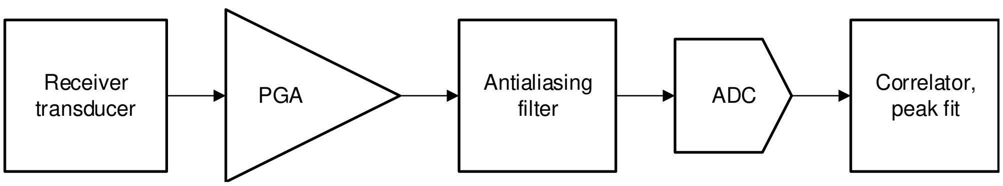

Figure 2-2. Block Diagram for Correlation-Based Differential TOF Estimator

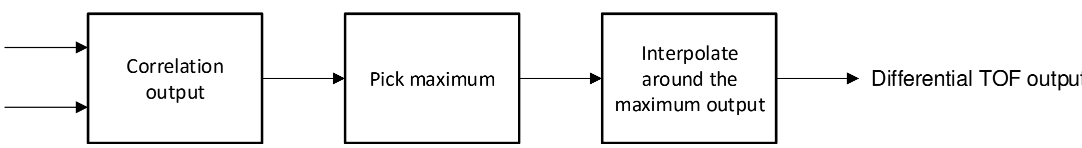

Figure 2-3. Block Diagram of Signal Processing for Differential TOF Measurement Using the Correlation Method

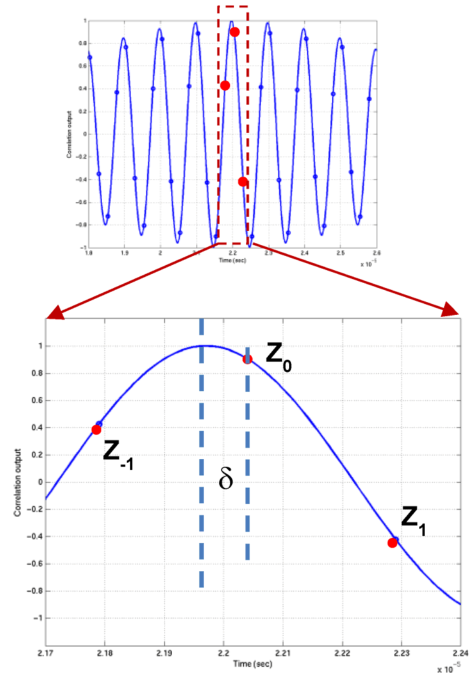

Figure 2-4. Interpolation Step in the ADC-Based Correlation Technique for Differential TOF Estimation

Efficient interpolation techniques have been given in Reference [4]. As previously mentioned, for efficiency of implementation, the correlation is computed over few points leading to a low-power implementation.

To ensure that Z_0 is the maximum point, the correlation peak runs through a search algorithm sequentially computing the three adjacent correlation terms (Z_{-1}, Z_0, and Z_{+1}) until it finds the maximum Z_0 that is larger than Z_{-1} and Z_{+1} and the earlier correlation terms. The search window for finding the correlation peak can be set using USS_ALG_NUM_CYCLES_SEARCH_CORR in USS_userConfig.h or ussAlgConfig.numCycleSearchCorrPeak. Typically, only an additional 1 or 2 adjacent correlation points are computed in addition to the 3 correlation points.

2.2 Absolute Time-of-Flight (AbsTOF) Measurement (T_{up} and T_{dn})

As given in Section 1.1.2, estimating an accurate absolute time of flight in water means that a temperature sensor is not needed to compute the velocity of sound in water. Given that the whole signal waveform is captured using an ADC, there are different algorithms that can be used to calculate the AbsTOF. The following section describes two algorithms, one that is implemented as part of the USS Software Library and one that is planned to be implemented as part of the future releases of the USS Software Library.

2.2.1 AbsTOF Calculation

The absolute time of flight (AbsToF) is determined by a two-stage process, namely acquisition and tracking. The acquisition process is implemented when there is no previous memory of the absTOF value (for example during the first signal capture) or when the algorithm detects an anomaly in two consecutive measurements of AbsTOF. The acquisition process algorithm consumes more power, so it is not implemented during each measurement. Instead, the tracking algorithm is implemented during each measurement.

2.2.1.1 Acquisition Algorithm for AbsTOF

As mentioned above, the acquisition algorithm is run when there is no previous memory of the AbsTOF value or when the algorithm detects an anomaly in two consecutive measurements of AbsTOF. Figure 2-5 shows a representative captured ADC waveform. The small circles in this figure represent the captured points.

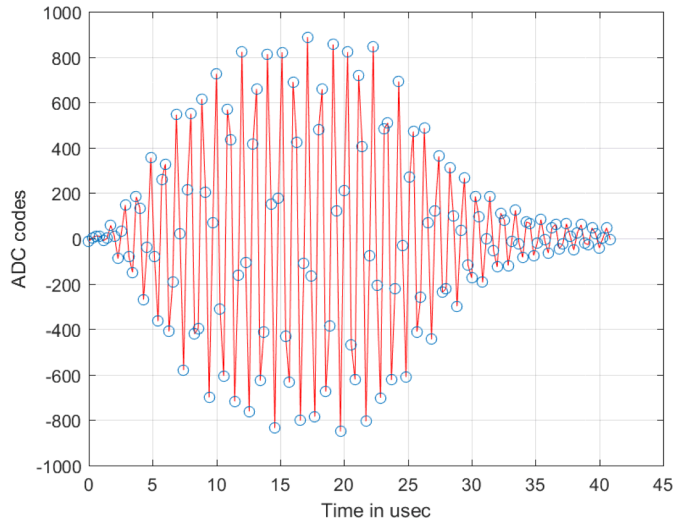

Figure 2-5. Representative Captured Waveform

As given in Equation 8, i is the time index for the signal capture and $\overline{r}_1 = \{r_1^1, r_1^2, r_1^3, \ldots, r_1^N\}$ is the upstream captured signal.

The acquisition algorithm then employs the following steps:

1. For every i equal to 2 to (N – 1), let i = {i_1, i_2, ..., i_M } for which $r_1^{i-1} \le r_1^i$ and $r_1^{i+1} \le r_1^i$.

   This means the central value r_1^i is greater than or equal to the two points on either side. The algorithm then uses parabolic interpolation between the $\{r_1^{i-1}, r_1^i, r_1^{i+1}\}$ for all such i. A parabolic interpolation is chosen (rather than the cosine interpolation for dTOF calculation) for reduced complexity, and the accuracy on AbsTOF estimation is not as tight as the dTOF estimation in terms of contribution to the overall flow error. The algorithm tabulates all these interpolated values. Letting $\tilde{r}$ denote the interpolated value these tabulated values can be given by $\{\tilde{r}_1^{i_1}, \tilde{r}_1^{i_2}, \ldots, \tilde{r}_1^{i_M}\}$. These interpolated values would now correspond to the "maximum of lobe" values of each wave in Figure 2-5. These are shown by dark red dots in Figure 2-6 and Figure 2-7.
2. The algorithm then computes the maximum over all these tabulated values $\{\tilde{r}_1^{i_1}, \tilde{r}_1^{i_2}, \ldots, \tilde{r}_1^{i_M}\}$. This thus generates the maximum of the signal. Let this maximum of the signal be denoted by $\overline{r}_1^{max}$.
3. Let η denote the threshold for the wave lobe that we would like the AbsTOF algorithm to lock on to. This threshold would be a function of the type of transducers and should be set to a value where we expect the maximum rate of the change of the waveform. This threshold is typically set to 0.1 in the USS Software Library. Then let $\eta^{thresh} = \eta \times \overline{r}_1^{max}$. This threshold can be controlled using the #define USS_ALG_RATIO_OF_TRACK_LOBE in USS_userConfig.h and maintained in USS_Algorithms_User_Configuration. ratioOfTrackLobeToPeak.
4. For the tabulated interpolated values $\{\tilde{r}_1^{i_1}, \tilde{r}_1^{i_2}, \ldots, \tilde{r}_1^{i_M}\}$, find that value of i = i_K for which the tabulated value is closest to η^{thresh} that is the $abs\left(\eta^{thresh} - \tilde{r}_1^{i_K}\right)$ is minimum. The offset delay of the maximum from index i_K is then calculated from the parabolic interpolation equation.

   The value i_K would now be used as an index for the next signal capture. Figure 2-6 and Figure 2-7 show the acquisition process.

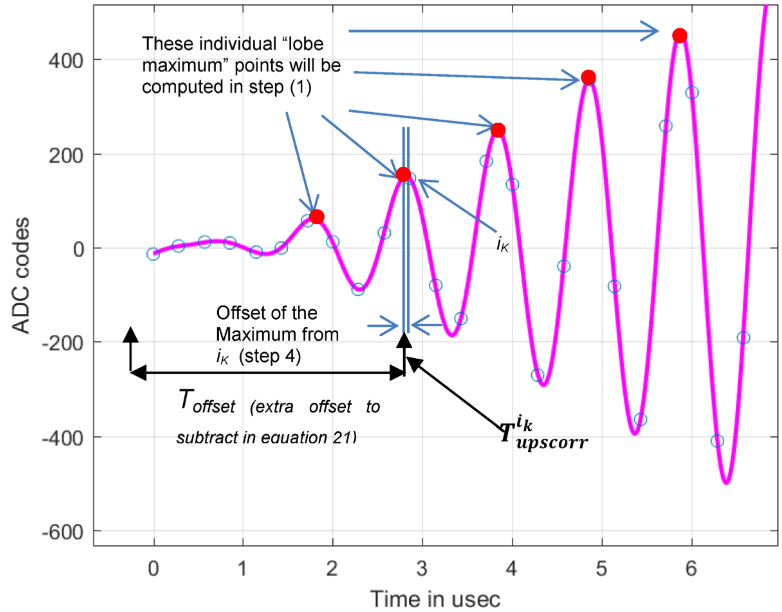

Figure 2-6. Interpolation in Acquisition Algorithm of AbsTOF

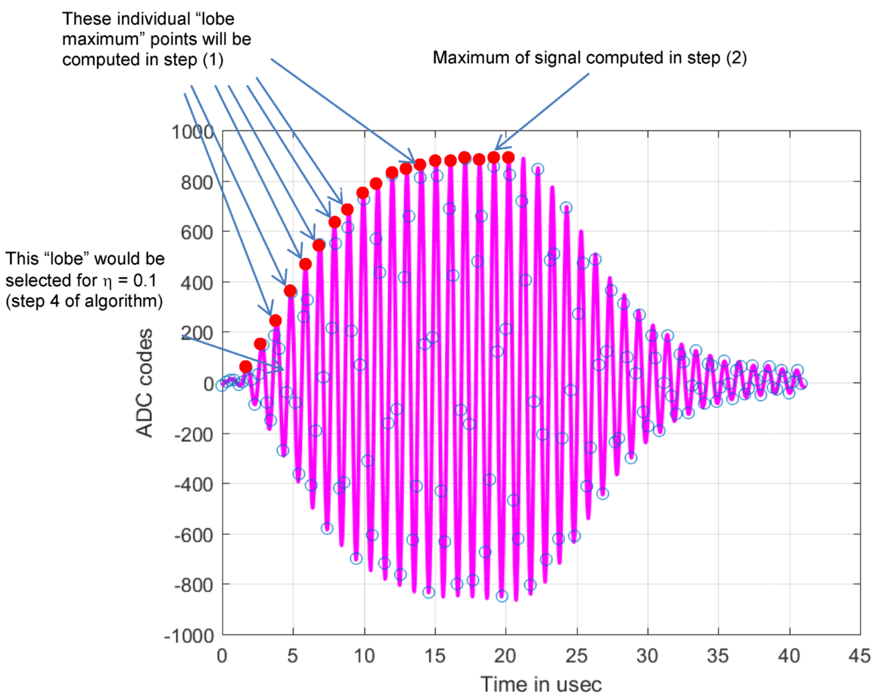

Figure 2-7. Data Points for Acquisition Algorithm for AbsTOF

2.2.1.2 Tracking Algorithm for AbsTOF

Let i_K denote the index from the previous capture (the procedure to get this during acquisition was described in Section 2.2.1.1) for previous burst j–1 and let j denote the current capture. Now, the algorithm has the following steps:

1. The algorithm checks if $r_1^{i_k-1} \leq r_1^{i_k}$ and $r_1^{i_k+1} \leq r_1^{i_k}$, if this is not true then it follows steps (2) and (3). If it is true, then the algorithm goes to step (4).
2. If however $r_1^{i_k-1} > r_1^{i_k}$ then i_k is set equal to i_k–1 and if $r_1^{i_k+1} > r_1^{i_k}$ then i_k is set equal to i_k+1.
3. The check in step (1) is now repeated on this new index i_K. In the water flow meter USS Software Library, a maximum of one such update in step (2) is allowed. If the algorithm still does not satisfy the inequality in step (1) then a full acquisition as in Section 2.2.1.1 is triggered.
4. The offset delay of the maximum from index i_K is then calculated from the parabolic interpolation equation.

   $T_{upscorr}^{i_k}$ denotes the effective time.

The upstream absolute time of flight is thus given by Equation 13.

$$T_{ups}^{abs} = T_{prop} + T_{upscorr}^{i_k} - T_{offset} \tag{13}$$

In this equation, T_{proop} is the propagation time that is specified using `#define USS_ACOUSTIC_LENGTH` in USS_userConfig.h and is maintained in USS_Meter_Configuration.acousticLength as part of the application meter configuration. It corresponds to the approximate propagation time for ultrasound in the given meter. Typically T_{proop} is 35 to 40 µs. T_{offset} corresponds to the number of cycles to back track from the lobe corresponding to the index i_K and is a function of the threshold η. In the USS Software Library, T_{offset} is set to 5 µs and can be modified using the user configuration `#define USS_ALG_ADC_ADDITIONAL_CAP_DLY`. It is maintained in the variable USS_Algorithms_User_Configuration.ADCAdditionalCaptureDelay.

The calculations of acquisition and tracking for the upstream direction are repeated for the downstream direction. The software keeps track of another index i_K for the downstream data for each burst j.

3 References

1. National Physical Labs (NPL), Underwater Acoustics, Technical Guides - Speed of Sound in Pure Water http://resource.npl.co.uk/acoustics/techguides/soundpurewater/speedpw.pdf
2. D.Marioli, C.Narduzzi, C.Offelli, D.Petri, E.Sardini, A.Taroni, Digital time of flight for ultrasonic sensors, IEEE Transactions on Instrumentation and Measurement, Vol. 41, No. 1, February 1992
3. Charles Knapp, Clifford Carter, The generalized correlation method for estimation of time delay, IEEE Transactions on Acoustics, Speech and Signal Processing, No. 4, August 1976
4. A Comparison of Time Delay Estimation Methods for Periodic Signals, Travis Wiens, Stuart Bradley, IEEE Transactions on Instrumentation and Measurement, Vol. 41, No. 1, February 1992

4 Revision History

NOTE: Page numbers for previous revisions may differ from page numbers in the current version.

Changes from March 4, 2019 to July 15, 2021 **Page**

- Updated the numbering format for tables, figures, and cross references throughout the document.................. 1
- Corrected a typo in Equation 9 4
- Corrected equation formatting in Section 2.2.1.1, *Acquisition Algorithm for AbsTOF* 6